Robust Output Regulation for a Planar Two-Link Robotic Manipulator ⋆

Eduardo S. Saraiva * **Aurélio T. Salton** * **Jeferson V. Flores** *
Rafael S. Castro **

* *Faculdade de Engenharia Elétrica, Universidade Federal do Rio
Grande do Sul, RS.*
** *Escola Politécnica, Pontifícia Universidade Católica do Rio Grande
do Sul, RS.*

Abstract: This paper deals with the problem of robust output regulation of planar two degrees of freedom robotic manipulators. An internal model controller is synthesized by a systematic framework that considers polynomial mappings of the steady-state trajectory. The closed-loop stabilization is guaranteed by using a descriptor differential-algebraic representation of the system. This methodology allows the controller design problem to be cast as a convex optimization problem subject to linear matrix inequalities.

Resumo: Este artigo trata do problema de regulação robusta de saída de manipuladores robóticos planares de dois graus de liberdade. Um modelo interno é sintetizado através de um procedimento sistemático que considera mapeamentos polinomiais das trajetórias de regime permanente. A estabilização em malha fechada é garantida pelo uso de uma representação algébrica-diferencial descriptora do sistema. Esta metodologia permite a representação do problema de projeto do controlador por um problema de otimização convexa sujeito a desigualdades matriciais lineares.

Keywords: Output Regulation, Internal Model, Linear Matrix Inequalities, Differential-Algebraic Representation.

Palavras-chaves: Regulação de Saída, Modelo Interno, Desigualdades Matriciais Lineares, Representação Algébrica-Diferencial.

1. INTRODUCTION

The robotic manipulator control problem is a classic subject in the field of control engineering. The interest in this system comes from the fact that the control design can be a challenging task due to the nonlinear multivariable characteristics intrinsic to the model, as well as the uncertainties of parameters. Moreover, the applications where robotic manipulators are present grow every day to aid the industrial sector and substitute human collaborators in risky tasks.

One can find a diversity of control techniques for robotic manipulator systems. For example, Yi and Zhai (2019) presents a sliding mode controller for trajectory tracking even in the presence of external disturbances and uncertain parameters. In Chen et al. (2018) a model-assisted extended state observer combined with the computed torque technique is presented to guarantee robustly tracking control. Fractional order fuzzy PID controllers are studied in Kumar et al. (2020), Kumar et al. (2018) and Muñoz-Vázquez et al. (2019).

To contribute to the above-mentioned literature, this paper proposes a systematic framework to track reference signals focused on robotic manipulator applications with uncertain parameters. Assuming the reference signal described by an autonomous exosystem, the robust output regulation theory can be applied to obtain a dynamic controller (internal model) capable to provide the necessary signals to achieve null tracking error in steady-state (Isidori et al., 2003). To the systems where an exact steady-state solution can not be achieved a practical output regulation framework can be accomplished as presented in Castro et al. (2022). Once the steady-state conditions are established this paper has targeted the design of a stabilizing controller that will lead the system states to the steady-state manifold (Castro, 2019). To achieve this goal, the controller design can be cast as a convex optimization problem through the descriptor differential-algebraic representation (Saraiva et al., 2020). The main advantages of this approach are 1. robustness of the solution employing a small-gain smooth controller, 2. the possibility to accommodate nonlinearities instead of canceling them, 3. theoretical guarantees for the practical output regulation, and 4. a systematic stabilization design based on the solution of linear matrix inequalities.

2. PRELIMINARS

2.1 Problem Formulation

A planar two-link manipulator can be seen as a rigid body where each link influences the entire manipulator motion.

This chain of motion can be described by a model as follows:

$$M(\boldsymbol{\theta})\,\dot{\boldsymbol{\omega}} + \mathbf{v}(\boldsymbol{\theta},\boldsymbol{\omega}) = \mathbf{u} \qquad (1)$$

where $\boldsymbol{\theta} \in \mathbb{R}^2$ is the angle joints vector, $\boldsymbol{\omega} = \dot{\boldsymbol{\theta}} \in \mathbb{R}^2$ is the angular velocity vector, $\mathbf{u} \in \mathbb{R}^2$ is the input torque for the respective joint. Moreover, $\mathbf{v}(\boldsymbol{\theta},\boldsymbol{\omega}) \in \mathbb{R}^2$ is the vector of Coriolis and centrifugal effects, that can be described by:

$$\mathbf{v}(\boldsymbol{\theta},\boldsymbol{\omega}) = a_1 \sin(\theta_2) \begin{bmatrix} -\omega_2^2 - 2\omega_1\omega_2 \\ \omega_1^2 \end{bmatrix}, \qquad (2)$$

$M(\boldsymbol{\theta}) \in \mathbb{R}^{2\times 2}$ is the system inertia matrix given by:

$$M(\boldsymbol{\theta}) = \begin{bmatrix} a_2 + 2a_1\cos(\theta_2) + a_3 & a_2 + a_1\cos(\theta_2) \\ a_2 + a_1\cos(\theta_2) & a_2 \end{bmatrix}, \qquad (3)$$

the variables a_1, a_2 and a_3 are related to the link mass m_i and lenght l_i, $i = 1, 2$, as follows:

$$a_1 = \ell_1\ell_2 m_2; \ a_2 = \ell_2^2 m_2; \ a_3 = \ell_1^2(m_1 + m_2). \qquad (4)$$

Furthermore, the system has an uncertain parameter related to the mass in the manipulator end-effector, given by:

$$m_2 = \bar{m}_2 + \delta_m \qquad (5)$$

where $\bar{m}_2$ represents the nominal mass of the link 2 and δ_m represents the unknown but bounded mass carried by the manipulator end-effector. Figure 1 presents the two-link planar manipulator schematic. The problem to be
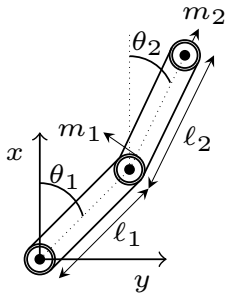
Figure 1. Schematic of two-link planar robotic manipulator.

addressed in this paper is the design of a robust controller such that the system (1) can track the dynamic reference given by:

$$\begin{aligned} r_1 &= \varrho_1 \sin(\omega_f t + \rho_1), \\ r_2 &= \varrho_2 \sin(\omega_f t + \rho_2), \end{aligned} \qquad (6)$$

where $\omega_f \in \mathbb{R}$ is the frequency of the reference signal, $\varrho_{1,2} \in \mathbb{R}$ is the signal amplitude, and $\rho_{1,2} \in \mathbb{R}$ is the signal phase.

2.2 Robust Output Regulation

To illustrate the foundations of the Robust Output Regulation theory presented in (Isidori et al., 2003) let us consider a nonlinear system given by:

$$\begin{cases} \dot{\mathbf{x}} = f(\mathbf{x}, \mathbf{w}, \mathbf{u}) \\ \mathbf{y} = g(\mathbf{x}, \mathbf{w}) \\ \mathbf{e} = h(\mathbf{x}, \mathbf{w}) \end{cases} \qquad (7)$$

where $\mathbf{x} \in \mathbb{R}^{n_x}$ is the control input, $\mathbf{y} \in R^{n_y}$ denote the plant measurements, $\mathbf{e} \in R^{n_e}$ is the output error and

$\mathbf{w} \in R^{nu}$ is a vector of exogenous states generated by an autonomous exosystem of the form:

$$\dot{\mathbf{w}} = s(\mathbf{w}) \ . \qquad (8)$$

Finally, assume the following nonlinear output feedback controller:

$$\begin{cases} \dot{\boldsymbol{\eta}} = \phi(\boldsymbol{\eta}, \mathbf{y}) \\ \mathbf{u} = \theta(\boldsymbol{\eta}, \mathbf{y}) \end{cases} \qquad (9)$$

where $\boldsymbol{\eta} \in \mathbb{R}^{n_\eta}$ is the controller state vector.

The closed-loop system (7),(8) and (9) for all initial conditions $(\mathbf{x}(0), \boldsymbol{\eta}(0), \mathbf{w}(0)) \in \mathcal{X} \subseteq \mathbb{R}$ is said to:

- be bounded if $\exists\, \epsilon_1, \epsilon_2, \epsilon_3 > 0$ such that:

$$||\mathbf{x}(t)|| < \epsilon_1, \ ||\boldsymbol{\eta}(t)|| < \epsilon_2, ||\mathbf{w}(t)|| < \epsilon_3, \forall t > 0; \quad (10)$$

- achieves asymptotic output regulation if the trajectories are bounded and:

$$\lim_{t\to\infty} ||\mathbf{e}(t)|| = 0; \qquad (11)$$

- achieves ε-practical output regulation, for some ultimate error bound $\varepsilon \geq 0$ if the trajectories are bounded and also:

$$\lim_{t\to\infty} ||\mathbf{e}(t)|| \leq \varepsilon. \qquad (12)$$

Given the conditions presented above, the aim is to design controller functions $\phi(\boldsymbol{\eta}, \mathbf{y})$ and $\theta(\boldsymbol{\eta}, \mathbf{y})$ such that the closed-loop system achieves output regulation under the following assumption:

Assumption 1. There exists a compact invariant set $\mathcal{W}_0 \in \mathbb{R}^{n_w}$ such that:

$$\mathbf{w}(0) \in \mathcal{W}_0 \to w(t) \in \mathcal{W}_0, \forall t \neq 0 \qquad (13)$$

To design these controller functions let us suppose the existence of steady-state mappings $\boldsymbol{\pi}(\mathbf{w}) : \mathcal{W}_0 \to \mathbb{R}^{n_x}$, $\boldsymbol{\sigma}(\mathbf{w}) : \mathcal{W}_0 \to \mathbb{R}^{n_\eta}$, $\mathbf{u}(\mathbf{w}) : \mathcal{W}_0 \to \mathbb{R}^{n_u}$ and $\mathbf{y}(\mathbf{w}) : \mathcal{W}_0 \to \mathbb{R}^{n_y}$ satisfying: $\boldsymbol{\pi}(0) = 0$, $\boldsymbol{\sigma}(0) = 0$, $\mathbf{y}(0) = 0$, $\mathbf{u}(0) = 0$ such that

$$\begin{cases} \mathcal{L}_{s(\mathbf{w})}\boldsymbol{\pi}(\mathbf{w}) = f(\boldsymbol{\pi}(\mathbf{w}), \mathbf{w}, \mathbf{u}(\mathbf{w}))) \\ \mathbf{y}(\mathbf{w}) = g(\boldsymbol{\pi}(\mathbf{w}), \mathbf{w}) \\ \mathbf{e}(\mathbf{w}) = h(\boldsymbol{\pi}(\mathbf{w}), \mathbf{w}) \end{cases} \qquad (14)$$

$$\begin{cases} \mathcal{L}_{s(\mathbf{w})}\boldsymbol{\sigma}(\mathbf{w}) = \phi(\boldsymbol{\sigma}(\mathbf{w}), \mathbf{d}(\mathbf{w})) \\ \mathbf{u}(\mathbf{w}) = \theta(\boldsymbol{\sigma}(\mathbf{w}), \mathbf{d}(\mathbf{w})) \end{cases} \qquad (15)$$

Given the above mappings, it is the task of controller (9) to achieve,

$$(\mathbf{x}(0), \boldsymbol{\eta}(0), \mathbf{w}(0)) \in \mathcal{X} \to \begin{cases} \lim_{t\to\infty} ||\mathbf{x}(t) - \boldsymbol{\pi}(\mathbf{w}(t))|| = 0 \\ \lim_{t\to\infty} ||\boldsymbol{\eta}(t) - \boldsymbol{\sigma}(\mathbf{w}(t))|| = 0 \end{cases} \qquad (16)$$

such that the closed loop system may achieve asymptotic output regulation or where $\mathbf{e}(\mathbf{w}) \neq 0$ it verifies that

$$\lim_{t\to\infty} ||\mathbf{e}(t)|| \leq \varepsilon = sup||\mathbf{e}(\mathbf{w})|| \qquad (17)$$

thus, the system trajectories achieve ε-practical output regulation for all initial conditions in $\mathcal{X}$.

To achieve this goal the powerful technique of the internal model principle can be used (Isidori et al., 2003). This methodology relies on the actual controller dynamics to reconstruct the steady-state control input. A proper internal model controller is achieved when the controller functions are satisfying the regulator equations (14) and (15).

Before designing an internal model function, the following steps must be followed in order to construct the steady state mappings $\boldsymbol{\pi}(\mathbf{w})$ and $\boldsymbol{\sigma}(\mathbf{w})$. First, it is necessary to establish the system steady-state for the ideal case where $e(w) = 0$, this can be done by the following procedure:

$$\begin{cases} \mathbf{e} = \mathbf{f}_0(\mathbf{w}) + \mathbf{b}_0(\mathbf{w})\,\mathbf{x}_1 \\ \dot{\mathbf{x}}_1 = \mathbf{f}_1(\mathbf{x}_1, \mathbf{w}) + \mathbf{b}_1(\mathbf{x}_1, \mathbf{w})\,\mathbf{x}_2 \\ \quad\vdots \\ \dot{\mathbf{x}}_n = \mathbf{f}_n(\mathbf{x}_1, \ldots, \mathbf{x}_n, \mathbf{w}) + \mathbf{b}_n(\mathbf{x}_1, \ldots, \mathbf{x}_n, \mathbf{w})\,\mathbf{u} \end{cases} \quad (18)$$

In this scenario, $\boldsymbol{\pi}(\mathbf{w})$ and $\mathbf{u}(\mathbf{w})$ can be recursively obtained for any exosystem function $s(\mathbf{w})$ according to

$$\begin{cases} \boldsymbol{\pi}_1(\mathbf{w}) = -\mathbf{b}_0^{-1}(\mathbf{w})\,\mathbf{f}_0(\mathbf{w}) \\ \boldsymbol{\pi}_2(\mathbf{w}) = -\mathbf{b}_1^{-1}(\boldsymbol{\pi}_1(\mathbf{w}), \mathbf{w})\left(\mathbf{f}_1(\boldsymbol{\pi}_1(\mathbf{w}), \mathbf{w}) - \mathcal{L}_{s(\mathbf{w})}\boldsymbol{\pi}_1(\mathbf{w})\right) \\ \quad\vdots \\ \mathbf{u}(\mathbf{w}) = -\mathbf{b}_n^{-1}(\boldsymbol{\pi}(\mathbf{w}), \mathbf{w})\left(\mathbf{f}_n(\boldsymbol{\pi}(\mathbf{w}), \mathbf{w}) - \mathcal{L}_{s(\mathbf{w})}\boldsymbol{\pi}_n(\mathbf{w})\right) \end{cases} \quad (19)$$

assuming that $\mathbf{b}_i^{-1}(\mathbf{w}), i = 0 \cdots n$ are non-singular $\forall\, \mathbf{w} \in \mathcal{W}$.

Once the the steady-states mappings $\boldsymbol{\pi}(\mathbf{w})$ and $\mathbf{u}(\mathbf{w})$ are obtained the so-called generalized immersion approach can be used to robustly generate the steady-state control input $\mathbf{u}(\mathbf{w})$. This approach assumes the existence of a function $\zeta(\cdot)$ that satisfies the following relation for some natural number N (Chen and Huang, 2015):

$$\mathcal{L}_{s(\mathbf{w})}^N \mathbf{u}(\mathbf{w}) = \zeta(\mathbf{u}(\mathbf{w}), \mathcal{L}_{s(\mathbf{w})}\mathbf{u}(\mathbf{w}), \ldots, \mathcal{L}_{s(\mathbf{w})}^{N-1}\mathbf{u}(\mathbf{w})) \quad (20)$$

The function $\zeta(\cdot)$ is capable of reconstructing an internal model controller signal considering a harmonic exogenous system with a linear internal model which satisfies the second condition for the regulator equations (15) through the following:

$$\begin{cases} \mathbf{u} = \boldsymbol{\eta}_1 + \boldsymbol{\kappa}(\boldsymbol{y}) \\ \dot{\boldsymbol{\eta}}_1 = \boldsymbol{\eta}_2 + \boldsymbol{\gamma}_1(\boldsymbol{y}) \\ \dot{\boldsymbol{\eta}}_2 = \boldsymbol{\eta}_3 + \boldsymbol{\gamma}_2(\boldsymbol{y}) \\ \quad\vdots \\ \dot{\boldsymbol{\eta}}_N = \zeta(\boldsymbol{\eta}_1, \boldsymbol{\eta}_2, \ldots, \boldsymbol{\eta}_N) + \boldsymbol{\gamma}_N(\boldsymbol{y}) \end{cases} \quad (21)$$

where $\kappa, \gamma_1, \ldots, \gamma_N$ are free functions used to guarantee closed-loop stabilization, provided they evaluate as zero in steady-state. The steady-state trajectory of the controller is given by:

$$\begin{cases} \boldsymbol{\eta}_1(\mathbf{w}) = \mathbf{u}(\mathbf{w}) \\ \boldsymbol{\eta}_2(\mathbf{w}) = \mathcal{L}_{s(\mathbf{w})}\mathbf{u}(\mathbf{w}) \\ \boldsymbol{\eta}_3(\mathbf{w}) = \mathcal{L}_{s(\mathbf{w})}^2\mathbf{u}(\mathbf{w}) \\ \quad\vdots \\ \boldsymbol{\eta}_N(\mathbf{w}) = \mathcal{L}_{s(\mathbf{w})}^{N-1}\mathbf{u}(\mathbf{w}) \end{cases} \quad (22)$$

The objective is recast as that of determining a function $\zeta(\cdot)$ that satisfies relation (20), and the free terms in (21) that satisfy (16).

Note that if the exosystem is linear with imaginary eigenvalues and the steady-state control input $\mathbf{u}(\mathbf{w})$ is a polynomal function of finite degree, then the function $\zeta(\cdot)$ can be described as

$$\zeta(\eta_1, \ldots, \eta_N) = -a_0\eta_1 - a_1\eta_2 - \cdots - a_{N-1}\eta_N \quad (23)$$

To obtain coefficients $a_0, \ldots, a_{N-1}$ it is possible to rewrite the steady-state control input via a complex Fourier series, such as

$$\mathbf{u}(\mathbf{w}(t)) = \sum_{i=1}^N c_i(\mathbf{w}(0))e^{\lambda_i t} \quad (24)$$

for some coefficients $c_1, \ldots, c_N$ and harmonics λ_i. So, it follows that $a_0, \ldots, a_{N-1}$ can be designed in a way such that the polynomial function $\lambda^N + a_{N-1}\lambda^{N-1} + \cdots + a_1\lambda + a_0$ has roots equal to the harmonics $\{\lambda_1, \ldots, \lambda_N\}$ (Castro et al., 2022).

3. MAIN RESULTS

This section is intended to adapt the theory revisited in the previous section to the 2 DOF planar manipulator problem and provide a framework that is capable to achieve output regulation for this class of nonlinear systems. To do so, this section is divided into two subsections. The first one is focused on obtaining the system's closed-loop practical stability and designing the internal model controller. The second one addresses the problem of designing the stabilizing components that will lead the system trajectories towards the target steady-state manifold.

3.1 Internal Model Controller

First of all, it is necessary to establish the steady-state control signal that will be reconstructed by the internal model approach. Notice that system (1) can be described as (7) with $\mathbf{x} = \begin{bmatrix} \boldsymbol{\theta}^T & \boldsymbol{\omega}^T \end{bmatrix}^T$. Moreover, let us rewrite the reference signal and the uncertainty present in system (1) as the exogenous system present in (8):

$$s(\mathbf{w}) = \begin{cases} \dot{\mathbf{w}}_\theta = \omega_f \mathbf{w}_\omega \\ \dot{\mathbf{w}}_\omega = -\omega_f \mathbf{w}_\theta \\ \dot{\mathbf{w}}_m = 0 \end{cases} \quad (25)$$

where $\mathbf{r} = \mathbf{w}_\theta \in \mathbb{R}^2$ and $\mathbf{w}_\omega \in \mathbb{R}^2$ are the exogenous system reference signals and $\delta_m = \mathrm{w}_m \in \mathbb{R}$ represents the uncertain mass m_2 (1).

The output signal given by

$$\mathbf{y} = \mathbf{e} = \boldsymbol{\theta} - \mathbf{r}, \quad (26)$$

along with system (1) can be described as presented in (18) by the following variables:

$$\begin{array}{ll} \mathbf{f}_0 = -\mathbf{w}_\theta & \mathbf{b}_0 = I_2 \\ \mathbf{f}_1 = \mathbf{0}_2 & \mathbf{b}_1 = I_2 \\ \mathbf{f}_2 = -M(\mathbf{x}_1)^{-1}\mathbf{v}(\mathbf{x}_1, \mathbf{x}_2) & \mathbf{b}_2 = M(\mathbf{x}_1)^{-1}. \end{array} \quad (27)$$

Once the variables have been defined the steady-state mapping can be promptly obtained by the relation presented in (19):

$$\begin{aligned} \boldsymbol{\pi}_1(\mathbf{w}) &= \mathbf{w}_\theta \\ \boldsymbol{\pi}_2(\mathbf{w}) &= \omega_f \mathbf{w}_\omega. \end{aligned} \quad (28)$$

Through this methodology the steady-state control signal $\mathbf{u}(\mathbf{w})$ can be obtained as:

$$\mathbf{u}(\mathbf{w}) = -M(\boldsymbol{\pi}_1)\omega_f^2\boldsymbol{\pi}_1 + \mathbf{v}(\boldsymbol{\pi}_1, \boldsymbol{\pi}_2). \quad (29)$$

Notice that the signal $\mathbf{u}(\mathbf{w})$ can not be described by a polynomial function of finite degree due to the trigonometric terms present in matrix $M(\boldsymbol{\pi}_1)$ and vector $\mathbf{v}(\boldsymbol{\pi}_1, \boldsymbol{\pi}_2)$.

To obtain a function $\zeta(\cdot)$ able to reconstruct the internal model it is necessary to rewrite the trigonometric term using a Taylor series expansion. To do so, the following relation are used

$$\sin(\theta) = \sum_{h=0}^{p} (-1)^h \frac{\theta^{2h+1}}{(2h+1)!} \tag{30}$$

$$\cos(\theta) = \sum_{h=0}^{p} (-1)^h \frac{\theta^{2h}}{(2h)!}. \tag{31}$$

Where $h \in \mathbb{N}$ is the approximation order. This way, a approximation of the steady-state control input $\mathbf{u}(\mathbf{w})$ can be described as

$$\hat{\mathbf{u}}(\mathbf{w}) = -\hat{M}(\boldsymbol{\pi}_1)\omega_f^2 \boldsymbol{\pi}_1 + \hat{\mathbf{v}}(\boldsymbol{\pi}_1, \boldsymbol{\pi}_2). \tag{32}$$

where $\hat{M}(\boldsymbol{\pi}_1)$ and $\hat{\mathbf{v}}(\boldsymbol{\pi}_1, \boldsymbol{\pi}_2)$ are respectively the Inertia matrix and the Coriolis vector approximation for an arbitrary $0 \leq p < \infty$, with $p \in \mathbb{N}$.

In order to deal with the approximation presented in (32), lets consider the following relaxed form of the regulator equations (14) and (15) according to the following:

$$\begin{cases} \mathcal{L}_{s(\mathbf{w})}\hat{\boldsymbol{\pi}}(\mathbf{w}) = f(\hat{\boldsymbol{\pi}}(\mathbf{w}), \mathbf{w}, \hat{\mathbf{u}}(\mathbf{w})) - \Delta_f(\mathbf{w}) \\ \hat{\mathbf{y}}(\mathbf{w}) = g(\hat{\boldsymbol{\pi}}(\mathbf{w}), \mathbf{w}) \\ \hat{\mathbf{e}}(\mathbf{w}) = h(\hat{\boldsymbol{\pi}}(\mathbf{w}), \mathbf{w}) \end{cases} \tag{33}$$

$$\begin{cases} \mathcal{L}_{s(\mathbf{w})}\hat{\boldsymbol{\sigma}}(\mathbf{w}) = \phi(\hat{\boldsymbol{\sigma}}(\mathbf{w}), \hat{\mathbf{y}}(\mathbf{w})) - \Delta_\phi(\mathbf{w}) \\ \hat{\mathbf{u}}(\mathbf{w}) = \boldsymbol{\theta}(\hat{\boldsymbol{\sigma}}(\mathbf{w}), \hat{\mathbf{y}}(\mathbf{w})) \end{cases} \tag{34}$$

where $\Delta_f(\mathbf{w})$ and $\Delta_\phi(\mathbf{w})$ represents relaxations in the regulator constraints. Due to this relaxation, the previously presented steady-state maps will be treated as approximations.

By expanding the steady-state control input (32) it is possible to notice that the signal has only odd harmonics, wich means that the internal model can be designed such that the harmonics $\{\pm(2h+1), h = 1, 2, ..., p\}$ are roots of the polynomial function $\lambda^N + a_{N-1}\lambda^{N-1} + \cdots + a_1\lambda + a_0$ with $N = 2(p+1)$.

The internal model can now be designed as (23) to cancel the harmonics presented in signal (32), for example

$(p = 0)$

$$\overset{(4)}{\hat{\mathbf{u}}}(\mathbf{w}) = -9\omega_f^4 \hat{\mathbf{u}}(\mathbf{w}) - 10\omega_f^2 \overset{..}{\hat{\mathbf{u}}}(\mathbf{w}) \tag{35}$$

$(p = 1)$

$$\overset{(6)}{\hat{\mathbf{u}}}(\mathbf{w}) = -225\omega_f^6 \hat{\mathbf{u}}(\mathbf{w}) - 259\omega_f^4 \overset{..}{\hat{\mathbf{u}}}(\mathbf{w}) - 35\omega_f^2 \overset{(4)}{\hat{\mathbf{u}}}(\mathbf{w}). \tag{36}$$

In order to satisfy condition (15) it is possible to rewrite the controller presented in (9) as a dynamic error and state-feedback controller (Castro et al., 2022):

$$\begin{cases} \dot{\boldsymbol{\eta}} = \boldsymbol{\Phi}\boldsymbol{\eta} + \boldsymbol{\Gamma}\mathbf{e} \\ \mathbf{u} = \boldsymbol{\Theta}\boldsymbol{\eta} + K\mathbf{x} \end{cases}, \tag{37}$$

where $\boldsymbol{\Phi} \in \mathbb{R}^{n_\eta \times n_\eta}$, $\boldsymbol{\Gamma} \in \mathbb{R}^{n_\eta \times n_y}$ and $K \in \mathbb{R}^{n_u \times n_x}$ are free design matrices. Note that the relaxed conditions (34) can be re-expressed as

$$\begin{cases} \mathcal{L}_{s(\mathbf{w})}\hat{\boldsymbol{\sigma}}(\mathbf{w}) = \boldsymbol{\Phi}\hat{\boldsymbol{\sigma}}(\mathbf{w}) + \boldsymbol{\Gamma}\hat{\mathbf{e}}(\mathbf{w}) - \Delta_\phi(\mathbf{w}) \\ \hat{\mathbf{u}}(\mathbf{w}) = \boldsymbol{\Theta}\hat{\boldsymbol{\sigma}}(\mathbf{w}) + K\hat{\boldsymbol{\pi}}(\mathbf{w}) \end{cases} \tag{38}$$

Through this methodology, the control mapping $\hat{\mathbf{u}}(\mathbf{w})$ can be robustly generated by the controller. To the examples previously presented the design of the internal model terms $\boldsymbol{\Phi}$ and $\boldsymbol{\Gamma}$ can be achieved as follows:

$(p = 0)$

$$\boldsymbol{\Phi} = \begin{bmatrix} 0 & I_2 & 0 & 0 \\ 0 & 0 & I_2 & 0 \\ 0 & 0 & 0 & I_2 \\ -9\omega_f^4 I_2 & 0 & -10\omega_f^2 I_2 & 0 \end{bmatrix}, \boldsymbol{\Gamma} = \begin{bmatrix} 0 \\ 0 \\ 0 \\ I_2 \end{bmatrix} \tag{39}$$

$(p = 1)$

$$\boldsymbol{\Phi} = \begin{bmatrix} 0 & I_2 & 0 & 0 & 0 & 0 \\ 0 & 0 & I_2 & 0 & 0 & 0 \\ 0 & 0 & 0 & I_2 & 0 & 0 \\ 0 & 0 & 0 & 0 & I_2 & 0 \\ 0 & 0 & 0 & 0 & 0 & I_2 \\ -225\omega_f^6 I_2 & -259\omega_f^4 I_2 & 0 & -35\omega_f^2 I_2 & 0 \end{bmatrix}, \boldsymbol{\Gamma} = \begin{bmatrix} 0 \\ 0 \\ 0 \\ 0 \\ 0 \\ I_2 \end{bmatrix} \tag{40}$$

Our next step is to design the stabilizing conditions that will lead to the steady-state manifold. We will show how this is achievable by designing both K and $\boldsymbol{\Theta}$.

3.2 Design of Stabilizing Components

Now, let us introduce an error vector between the plant and controller states and the respective steady-state mappings as follows:

$$\mathbf{z} = \begin{bmatrix} \mathbf{z}_p \\ \mathbf{z}_c \end{bmatrix} \triangleq \begin{bmatrix} \mathbf{x} - \hat{\boldsymbol{\pi}}(\mathbf{w}) \\ \boldsymbol{\eta} - \hat{\boldsymbol{\sigma}}(\mathbf{w}) \end{bmatrix}. \tag{41}$$

Note that $\Delta_\phi(\mathbf{w}) = \boldsymbol{\Gamma}\hat{\mathbf{e}}(\mathbf{w})$ and the dynamics of the controller deviation can be expressed as follows:

$$\dot{\mathbf{z}}_c = \boldsymbol{\Phi}\boldsymbol{\eta} + \boldsymbol{\Gamma}\mathbf{e} - \boldsymbol{\Phi}\hat{\boldsymbol{\sigma}}(\mathbf{w}) - \boldsymbol{\Gamma}\hat{\mathbf{e}}(\mathbf{w}) + \Delta_\phi(\mathbf{w}) = \boldsymbol{\Phi}\mathbf{z}_c + \boldsymbol{\Gamma}\mathbf{e} \tag{42}$$

Also, the control input can be rearranged as:

$$\mathbf{u} = \boldsymbol{\Theta}(\mathbf{z}_c + \hat{\boldsymbol{\sigma}}(\mathbf{w})) + K(\mathbf{z}_p + \hat{\boldsymbol{\pi}}(\mathbf{w})) = \boldsymbol{\Theta}\mathbf{z}_c + K\mathbf{z}_p + \hat{\mathbf{u}}(\mathbf{w}) \tag{43}$$

Observe that the control input $\mathbf{u}$ is composed of two parts, the steady-state term $\hat{\mathbf{u}}(\mathbf{w})$ and the stabilizing components $v \in \mathbb{R}^m$ which can be defined as:

$$v \triangleq \boldsymbol{\Theta}\mathbf{z}_c + K\mathbf{z}_p = \mathbf{K}\mathbf{z}. \tag{44}$$

with $\mathbf{K} = [K \quad \boldsymbol{\Theta}]$.

The plant error dynamics can then be expressed as:

$$\begin{bmatrix} I & 0 \\ 0 & M(\mathbf{x}_1) \end{bmatrix} \begin{bmatrix} \dot{\mathbf{z}}_{p_1} \\ \dot{\mathbf{z}}_{p_2} \end{bmatrix} = \begin{bmatrix} \mathbf{z}_{p_2} \\ \mathbf{u} - \mathbf{v}(\mathbf{x}_1, \mathbf{x}_2) + M(\mathbf{x}_1)\omega_f^2\hat{\boldsymbol{\pi}}_1 \end{bmatrix} \tag{45}$$

By introducing the input signal (43) with (32) into the dynamics (45) results in

$$\begin{bmatrix} I & 0 \\ 0 & M(\mathbf{x}_1) \end{bmatrix} \begin{bmatrix} \dot{\mathbf{z}}_{p_1} \\ \dot{\mathbf{z}}_{p_2} \end{bmatrix} =$$

$$\begin{bmatrix} \mathbf{z}_{p_2} \\ v + (M(\mathbf{x}_1) - \hat{M}(\hat{\boldsymbol{\pi}}_1))\omega_f^2\hat{\boldsymbol{\pi}}_1 + \hat{\mathbf{v}}(\hat{\boldsymbol{\pi}}_1, \hat{\boldsymbol{\pi}}_2) - \mathbf{v}(\mathbf{x}_1, \mathbf{x}_2) \end{bmatrix} \tag{46}$$

Now let us consider a vector of time-varying parameters δ defined as:

$$\boldsymbol{\delta} = \begin{bmatrix} \sin(\theta_2) \\ \cos(\theta_2) \end{bmatrix} \in \mathbb{R}^2 \ , \tag{47}$$

Notice that the Coriolis vector $\mathbf{v}(\mathbf{x}_1, \mathbf{x}_2)$ can be written as a function of the error $\mathbf{z}$ and the reference $\mathbf{w}$ as follows:

$$\mathbf{v}(\mathbf{z}, \mathbf{w}) = a_1\delta_1 \begin{bmatrix} -(\hat{\pi}_4)^2 - 2(\hat{\pi}_3)(\hat{\pi}_4) \\ (\hat{\pi}_3) \end{bmatrix} + \\ a_1\delta_1 \begin{bmatrix} (z_4^2 + 2\hat{\pi}_4 z_4) + 2(z_3 z_4 + \hat{\pi}_4 z_3 + \hat{\pi}_3 z_4) \\ -(z_3^2 + 2\hat{\pi}_3 z_3) \end{bmatrix}. \tag{48}$$

The steady-state approximation Coriolis vector is given by:

$$\hat{\mathbf{v}}(\hat{\boldsymbol{\pi}}_1, \hat{\boldsymbol{\pi}}_2) = a_1 \sum_{h=0}^{p} (-1)^h \frac{\hat{\pi}_2^{2h+1}}{(2h+1)!} \begin{bmatrix} -(\hat{\pi}_4)^2 - 2(\hat{\pi}_3)(\hat{\pi}_4) \\ (\hat{\pi}_3) \end{bmatrix}. \tag{49}$$

This way, the difference between both Coriolis vector can be written as:

$$\hat{\mathbf{v}}(\hat{\boldsymbol{\pi}}_1, \hat{\boldsymbol{\pi}}_2) - \mathbf{v}(\mathbf{x}_1, \mathbf{x}_2) = \mathbf{v}_d + d_v \tag{50}$$

where

$$\mathbf{v}_d(\mathbf{z}, \hat{\boldsymbol{\pi}}, \boldsymbol{\delta}) = -a_1\delta_1 \begin{bmatrix} (z_4^2 + 2\hat{\pi}_4 z_4) + 2(z_3 z_4 + \hat{\pi}_4 z_3 + \hat{\pi}_3 z_4) \\ -(z_3^2 + 2\hat{\pi}_3 z_3) \end{bmatrix} \tag{51}$$

and

$$d_v(\hat{\boldsymbol{\pi}}, \boldsymbol{\delta}) = a_1 \left(\sum_{h=0}^{p} (-1)^h \frac{\hat{\pi}_2^{2h+1}}{(2h+1)!} - \delta_1 \right) \begin{bmatrix} -(\hat{\pi}_4)^2 - 2(\hat{\pi}_3)(\hat{\pi}_4) \\ (\hat{\pi}_3) \end{bmatrix} \tag{52}$$

Notice that vector (52) has no dependences of the error $\mathbf{z}$, this way, it can be treated as a residual dynamics associated to the Taylor series approximation.

Vector $\mathbf{v}_d(\mathbf{z}, \hat{\boldsymbol{\pi}}, \boldsymbol{\delta})$ can now be described as a function of the reference signal $\mathbf{w}$ as follows:

$$\mathbf{v}_d(\mathbf{z}, \mathbf{w}, \boldsymbol{\delta}) = -a_1\delta_1 \begin{bmatrix} (z_4^2 + 2\omega_f w_4 z_4) + 2(z_3 z_4 + \omega_f w_4 z_3 + \omega_f w_3 z_4) \\ -(z_3^2 + 2\omega w_3 z_3) \end{bmatrix}, \tag{53}$$

Furthermore, the trigonometric terms presented in the inertia matrix are described by $\boldsymbol{\delta}$ as well. For this reason, there is also a residual dynamics associated to the inertia matrix difference in (46) that can be described as

$$d_M(\hat{\boldsymbol{\pi}}, \boldsymbol{\delta}) = (M(\delta) - \hat{M}(\hat{\boldsymbol{\pi}}_1))\omega_f^2 \hat{\boldsymbol{\pi}}_1 \tag{54}$$

This way, the error dynamics can be fully described by the following equation:

$$\begin{bmatrix} I_2 & 0 & 0 \\ 0 & M(\boldsymbol{\delta}) & 0 \\ 0 & 0 & I_\eta \end{bmatrix} \begin{bmatrix} \dot{\mathbf{z}}_{p_1} \\ \dot{\mathbf{z}}_{p_2} \\ \dot{\mathbf{z}}_c \end{bmatrix} = \begin{bmatrix} \mathbf{z}_{p_2} \\ v + d + \mathbf{v}_d(\mathbf{z}, \mathbf{w}, \boldsymbol{\delta}) \\ \boldsymbol{\Phi}\mathbf{z}_c + \boldsymbol{\Gamma}\mathbf{z}_{p_1} \end{bmatrix} \tag{55}$$

where $d = d_M + d_v$. To design matrices $\boldsymbol{\Theta}$ and K such that the (55) is practical stable, the differential-algebraic representation (DAR) with descriptor components will be considered as follows (Saraiva et al., 2020):

$$\begin{cases} A_0\dot{\mathbf{z}} &= A_1\mathbf{z} + A_2(\mathbf{z}, \mathbf{w})\boldsymbol{\xi} + A_3(\boldsymbol{\delta})\dot{\mathbf{z}} + Bv + B_d d \\ 0 &= \Omega_1(\boldsymbol{\delta})\mathbf{z} + \Omega_2\boldsymbol{\xi} \end{cases} \tag{56}$$

The term $\boldsymbol{\xi} \in \mathbb{R}^{n_\xi}$ is a rational function, terms $A_1 \in \mathbb{R}^{n_z \times n_z}$, $A_2(\mathbf{z}, \mathbf{w}) \in \mathbb{R}^{n_z \times n_\xi}$, $B \in \mathbb{R}^{n_z \times n_u}$, $B_d \in \mathbb{R}^{n_z \times n_d}$, $\Omega_1(\boldsymbol{\delta}) \in \mathbb{R}^{n_\xi \times n_z}$ and $\Omega_2 \in \mathbb{R}^{n_\xi \times n_\xi}$ are affine matrix functions in $(\mathbf{z}, \boldsymbol{\delta})$, also $A_0 \in \mathbb{R}^{n_z \times n_z}$ and $A_3(\boldsymbol{\delta}) \in \mathbb{R}^{n_z \times n_z}$ contains the constant terms and the nonlinear terms that are multiplying $\dot{\mathbf{z}}$ respectively. The advantage of this framework is the capacity to design control problems by convex optimizations subject to linear matrix inequalities (LMIs) (Trofino and Dezuo, 2014).

Due to the nonlinearities present in vector (53) it is necessary to group the nonlinear terms in a new vector so the DAR representation can be achieved:

$$\boldsymbol{\xi} = [\Delta_1 z_4 \ \ \Delta_1 z_3]^T \tag{57}$$

where $\Delta_1 = a_1\delta_1$.

Due to the uncertainty present in m_2 let us consider the auxiliary variable as follows:

$$a_1 = \bar{a}_1 + \tilde{a}_1; \ a_2 = \bar{a}_1 + \tilde{a}_1; \ a_3 = \bar{a}_1 + \tilde{a}_1. \tag{58}$$

where $\bar{a}_j$ with $j = 1, 2, 3$, denotes the nominal components described as:

$$\bar{a}_1 = \ell_1\ell_2\bar{m}_2; \ \bar{a}_2 = \ell_2^2\bar{m}_2; \ \bar{a}_3 = \ell_1^2(m_1 + \bar{m}_2). \tag{59}$$

Followed by the uncertain parameters $\tilde{a}_j$ given by:

$$\tilde{a}_1 = \ell_1\ell_2 w_m; \ \tilde{a}_2 = \ell_2^2 w_m; \ \tilde{a}_3 = \ell_1^2 w_m. \tag{60}$$

Now, to obtain matrices A_0 and $A_3(\boldsymbol{\delta})$ it is necessary to rewrite the inertia matrix as:

$$M(\boldsymbol{\delta}) = \bar{M} + \tilde{M}(\boldsymbol{\delta}) \tag{61}$$

with

$$\bar{M} = \begin{bmatrix} \bar{a}_2 + \bar{a}_3 & \bar{a}_2 \\ \bar{a}_2 & \bar{a}_2 \end{bmatrix}, \tilde{M}(\boldsymbol{\delta}) = \begin{bmatrix} \tilde{a}_2 + \tilde{a}_3 + 2a_1\delta_2 & \tilde{a}_2 + a_1\delta_2 \\ \tilde{a}_2 + a_1\delta_2 & \tilde{a}_2 \end{bmatrix} \tag{62}$$

Given these definitions for $\mathbf{z}$, $\boldsymbol{\delta}$ and $\boldsymbol{\xi}$, the system (55) can be expressed in the descriptor DAR (56) with the following matrices:

$$A_0 = \begin{bmatrix} I_2 & 0 & 0 \\ 0 & \bar{M} & 0 \\ 0 & 0 & I_\eta \end{bmatrix}, A_3(\boldsymbol{\delta}) = \begin{bmatrix} 0 & 0 & 0 \\ 0 & \tilde{M}(\boldsymbol{\delta}) & 0 \\ 0 & 0 & 0 \end{bmatrix} \dot{\mathbf{z}}, B = \begin{bmatrix} 0_2 \\ I_2 \\ 0_\eta \end{bmatrix}$$

$$A_1 = \begin{bmatrix} 0 & I_2 & 0 \\ 0 & 0 & 0 \\ \boldsymbol{\Gamma} & 0 & \boldsymbol{\Phi} \end{bmatrix}, B_d = \begin{bmatrix} 0_2 \\ I_2 \\ 0_\eta \end{bmatrix}$$

$$A_2(\mathbf{z}, \mathbf{w}) = \begin{bmatrix} 0 & 0 \\ 0 & 0 \\ (z_4 + 2\omega_f w_4 + 2z_3 + 2\omega_f w_3) & 2\omega_f w_4 \\ 0 & -2z_3 - 2\omega_f w_3 \\ 0_{(\eta,1)} & 0_{(\eta,1)} \end{bmatrix}$$

$$\Omega_1(\boldsymbol{\delta}) = \begin{bmatrix} 0 & \Delta_1 \\ \Delta_1 & 0 \end{bmatrix}, \Omega_2 = \begin{bmatrix} -1 & 0 \\ 0 & -1 \end{bmatrix} \tag{63}$$

By now using an augmented vector $\boldsymbol{\xi}_a = [\boldsymbol{\xi}^T \ \ \dot{z}^T]^T \in \mathbb{R}^{n_{\xi_a}}$ that combines $\boldsymbol{\xi}$ with $\dot{z}$, we can show that the descriptor DAR from (56) can be re-arranged to appear as a traditional DAR introduced in Trofino and Dezuo (2014). In this case, it is necessary to include an extra constraint as follows:

$$0 = A_1\mathbf{z} + A_2(\mathbf{z}, \mathbf{w})\boldsymbol{\xi} + (A_3(\boldsymbol{\delta}) - A_0)\dot{z} + Bv + B_d d. \tag{64}$$

Moreover, since all of the descriptor nonlinearities were grouped into $A_3(\boldsymbol{\delta})\dot{z}$, it is possible to invert A_0 which is clearly non-singular from (63). This process allows the following representation:

$$\begin{cases} \dot{\mathbf{z}} = \mathbf{A_1}\mathbf{z} + \mathbf{A_2}(z, \mathbf{w}, \boldsymbol{\delta})\boldsymbol{\xi}_a + \mathbf{B}v + \mathbf{B}_d d \\ 0 = \boldsymbol{\Omega_1}(\boldsymbol{\delta})\mathbf{z} + \boldsymbol{\Omega_2}(z, \mathbf{w}, \boldsymbol{\delta})\boldsymbol{\xi}_a + \boldsymbol{\Omega_3}v + \boldsymbol{\Omega_4}d \end{cases}, \tag{65}$$

where the augmented matrices shown in here are constructed in the following manner:

$$\mathbf{A_1} = A_0^{-1}A_1 , \quad \mathbf{A_2}(z, \mathbf{w}, \boldsymbol{\delta}) = A_0^{-1}\left[A_2(\mathbf{z}, \mathbf{w})\ A_3(\boldsymbol{\delta})\right],$$

$$\boldsymbol{\Omega_1}(\boldsymbol{\delta}) = \begin{bmatrix} \Omega_1(\boldsymbol{\delta}) \\ A_1 \end{bmatrix}, \quad \boldsymbol{\Omega_2}(z, \mathbf{w}, \boldsymbol{\delta}) = \begin{bmatrix} \Omega_2 & 0 \\ A_2(\mathbf{z}, \mathbf{w}) & A_3(\boldsymbol{\delta}) - A_0 \end{bmatrix},$$

$$\mathbf{B} = A_0^{-1}B , \mathbf{B}_d = A_0^{-1}B_d , \boldsymbol{\Omega_3} = \begin{bmatrix} 0 \\ B \end{bmatrix}, \quad \boldsymbol{\Omega_4} = \begin{bmatrix} 0 \\ B_d \end{bmatrix} \tag{66}$$

It follows that closed-loop system can be written as

$$\begin{cases} \dot{\mathbf{z}} = (\mathbf{A_1} + \mathbf{BK})\mathbf{z} + \mathbf{A_2}(z, \mathbf{w}, \boldsymbol{\delta})\boldsymbol{\xi}_a + \mathbf{B}_d d \\ 0 = (\boldsymbol{\Omega_1}(\boldsymbol{\delta}) + \boldsymbol{\Omega_3}\mathbf{K})\mathbf{z} + \boldsymbol{\Omega_2}(z, \mathbf{w}, \boldsymbol{\delta})\boldsymbol{\xi}_a + \boldsymbol{\Omega_4}d \end{cases}, \tag{67}$$

A control law designed to the DAR representation (65) will only be valid within $\mathcal{X}$. By using level curves in a Lyapunov function $V(\mathbf{z})$ it is possible to find an estimate of the region of attraction of the closed loop system $\mathcal{R}$ that satisfy $\mathcal{R} \subset \mathcal{X}$. By choosing a quadratic Lyapunov function candidate $V(\mathbf{z}) = \mathbf{z}P\mathbf{z}$, it follows that an estimate for the region of attraction is given by

$$\mathcal{R} := \{\mathbf{z} : \mathbf{z}P\mathbf{z} \leq 1\}. \tag{68}$$

Also, due to the residual dynamics d, we cannot always drive the trajectories z(t) to zero, however it is possible to ensure they converge to a bounding terminal set $\mathcal{R}_d \subset \mathcal{R}$. Hence, $\mathcal{R}_d$ is a bounding set for the trajectories of the closed-loop system when subject to the residual dynamics $d \in \mathcal{D}$.

Let us define $\mathcal{D}$ and $\mathcal{R}_d$ as

$$\begin{aligned} \mathcal{D} &:= \left\{d \in \mathbb{R}^{n_d} : d^T R d \leq 1\right\} \\ \mathcal{R}_d &:= \left\{\mathbf{z} \in \mathbb{R}^{n_z} : \mathbf{z}^T P \mathbf{z} \leq \mu\right\} \end{aligned} \tag{69}$$

with $0 < \mu < 1$ such that $\mathcal{R}_d \subset \mathcal{R}$, and $R = R^T$.

Finally to showing our results it is also convenient to re-express the domain of interest $\mathcal{Z}$ in a standard polyhedral form such as

$$\mathcal{Z} = \left\{\mathbf{z} \in \mathbb{R}^{n_\mathbf{z}} : |\alpha_k \mathbf{z}_{pk}| \leq 1 , k = 1, 2, ..., n_\mathbf{z}\right\}, \tag{70}$$

$$\mathcal{W} = \left\{\mathbf{w} \in \mathbb{R}^5 : |\mathbf{w}_{1,2}| \leq \varrho, |\mathbf{w}_{3,4}| \leq \varrho, |\mathbf{w}_5| \leq \delta_m\right\}, \tag{71}$$

and

$$\Delta = \left\{\boldsymbol{\delta} \in \mathbb{R}^2 : |\delta_i| \leq 1, i = 1, 2\right\}. \tag{72}$$

Theorem 1. *Consider the system (55) and its DAR (65) subject to the control law (44). Suppose there exist a symmetric matrix $\hat{P} \in \mathbb{R}^{n_\mathbf{z} \times n_\mathbf{z}}$, matrices $\hat{L} \in \mathbb{R}^{n_{\boldsymbol{\xi}_a} \times n_{\boldsymbol{\xi}_a}}$ and $\hat{\mathbf{K}} \in \mathbb{R}^{n_\mathbf{u} \times n_\mathbf{z}}$ and scalars τ_1, τ_2 and μ such that:*

$$\hat{P} > 0, \tag{73}$$

$$\begin{bmatrix} 1 & \alpha_k \hat{P} \\ \star & \hat{P} \end{bmatrix} > 0 \ \forall k = 1, ..., n_\mathbf{z}, \tag{74}$$

$$\tau_2\mu > \tau_1 > 0, \ 1 > \mu > 0 \tag{75}$$

$$\text{He}\left\{\begin{bmatrix} \mathbf{A_1}\hat{P} + \tau_2\hat{P} + \mathbf{B}\hat{\mathbf{K}} & \mathbf{A_2}(z, \mathbf{w}, \boldsymbol{\delta})\hat{L} & \mathbf{B}_d \\ \boldsymbol{\Omega_1}(\boldsymbol{\delta})\hat{P} + \boldsymbol{\Omega_3}\hat{\mathbf{K}} & \boldsymbol{\Omega_2}(z, \mathbf{w}, \boldsymbol{\delta})\hat{L} & \boldsymbol{\Omega_4} \\ 0 & 0 & -\tau_1 R \end{bmatrix}\right\} < 0, \tag{76}$$

$\forall (z, \mathbf{w}, \boldsymbol{\delta}) \in \mathcal{V}(\mathcal{Z}) \times \mathcal{V}(\mathcal{W}) \times \mathcal{V}(\Delta)$ *. Then, all trajectories of system (55) with v in (44) and $\mathbf{K} = \hat{\mathbf{K}}\hat{P}^{-1}$ for all initial conditions* $\mathbf{z}(0)$ *starting in the region:*

$$\mathcal{R} = \{\mathbf{z} \in \mathbb{R}^{n_\mathbf{z}} : \mathbf{z}^\mathsf{T}\hat{P}^{-1}\mathbf{z} \leq 1\}. \tag{77}$$

enter the set $\mathcal{R}_d$ in finite time t_0 and remain there for all $t \geq t_0$ for $d \in \mathcal{D}$.

Proof: Consider a Lyapunov candidate function as:

$$V(\mathbf{z}) = \mathbf{z}^\mathsf{T}P\mathbf{z}, \tag{78}$$

with $P = P^T > 0$ in order to ensure that $V(\mathbf{z}) > 0 \ \forall \mathbf{z} \neq 0$. The derivative of (78) along the trajectories of (65) is given by:

$$\dot{V}(\mathbf{z}) = \begin{bmatrix} \mathbf{z}^\mathsf{T} & \boldsymbol{\xi}_a^\mathsf{T} & d^\mathsf{T} \end{bmatrix} \text{He}\left\{\begin{bmatrix} P(\mathbf{A_1} + \mathbf{BK}) & P\mathbf{A_2}(z, \mathbf{w}, \boldsymbol{\delta}) & P\mathbf{B}_d \\ 0 & 0 & 0 \\ 0 & 0 & 0 \end{bmatrix}\right\}\begin{bmatrix} \mathbf{z} \\ \boldsymbol{\xi}_a \\ d \end{bmatrix}. \tag{79}$$

Now, suppose the following inequality is satisfied for all $(\mathbf{z}, \boldsymbol{\delta}, \mathbf{w}) \in \mathcal{Z} \times \Delta \times \mathcal{W}$:

$$\dot{V}(\mathbf{z}) + 2\tau_1(1 - dRd) - 2\tau_2(\mu - \mathbf{z}P\mathbf{z}) +$$

$$\text{He}\left\{\boldsymbol{\xi}_a^\mathsf{T}L\left[\boldsymbol{\Omega_1}(\boldsymbol{\delta}) + \boldsymbol{\Omega_3}\mathbf{K}\ \boldsymbol{\Omega_2}(z, \mathbf{w}, \boldsymbol{\delta})\ \boldsymbol{\Omega_4}\right]\begin{bmatrix} \mathbf{z} \\ \boldsymbol{\xi}_a \\ d \end{bmatrix}\right\} < 0, \tag{80}$$

or equivalently:

$$\text{He}\left\{\begin{bmatrix} P(\mathbf{A_1} + \mathbf{BK}) + \tau_2 P & P\mathbf{A_2}(z, \mathbf{w}, \boldsymbol{\delta}) & P\mathbf{B}_d \\ L(\boldsymbol{\Omega_1}(\boldsymbol{\delta}) + \boldsymbol{\Omega_3}\mathbf{K}) & L\boldsymbol{\Omega_2}(z, \mathbf{w}, \boldsymbol{\delta}) & L\boldsymbol{\Omega_4} \\ 0 & 0 & -\tau_1 R \end{bmatrix}\right\} < 0. \tag{81}$$

Given that $\mu \geq 0$, $V(\mathbf{z}) > 0$ and $(\boldsymbol{\Omega_1} + \boldsymbol{\Omega_3}K)\mathbf{z} + \boldsymbol{\Omega_2}\boldsymbol{\xi}_a + \boldsymbol{\Omega_4}d = 0$, it follows that (80) implies that $\dot{V}(x) - 2\tau_1 d^T R d + 2\tau_2\mu\mathbf{z}^T P\mathbf{z} < 0$ and $\tau_1 - \tau_2\mu < 0 \ \forall (z, \mathbf{w}, \boldsymbol{\delta}) \in \mathcal{Z} \times \mathcal{W} \times \Delta$. Pre- and post-multiplying (81) by diag$\{P^{-1}, L^{-1}, I\}$, (76) is obtained, considering the change of variables $\hat{P} = P^{-1}$ and $\hat{L} = L^{-1}$. In the same way, the relation (73) is verified when pre- and post-multiplying $P > 0$ by P^{-1}.

To conclude the proof, if the LMI (76) is satisfied for $(z, \mathbf{w}, \boldsymbol{\delta})$ at the cartesian product of vertices $\mathcal{V}(\mathcal{Z}) \times \mathcal{V}(\mathcal{W}) \times \mathcal{V}(\Delta)$, by convexity they are also satisfied $\forall (z, \mathbf{w}, \boldsymbol{\delta}) \in \mathcal{Z} \times \mathcal{W} \times \Delta$. $\square$

From the domain of attraction estimate (77), it is concluded that minimizing the trace of $\hat{P}^{-1}$ implies the maximization of the sum of all semi-axes of the ellipsoidal set $\mathcal{R}$. Thus, the design of $\mathbf{K}$ that maximizes region $\mathcal{R}$ can be solved by the following convex optimization problem based on Theorem 1:

$$\begin{aligned} &\underset{N, \hat{P}, \hat{L}, \hat{K}}{\text{minimize}} && \text{tr}(N) \\ &\text{subject to} && (73), (83), (75), (76), \begin{bmatrix} N & I \\ \star & \hat{P} \end{bmatrix} > 0. \end{aligned} \tag{82}$$

Remark 1. It is possible to calculate the error ultimate bound ε after running the optimization problem (82). This calculation can be accomplished by the following matrix inequality:

$$\begin{bmatrix} \gamma & C\hat{P} \\ \star & \hat{P} \end{bmatrix} > 0 \tag{83}$$

where $\varepsilon = \sqrt{\gamma}$ and $C = [I_2\ 0]$.

Remark 2. It is important to note that no constraint has been imposed on the gain K, this may lead to extremely high gains when synthesizing the controller by numerical optimization. In order to circumvent this issue, it is suggested to consider the following design constraint:

$$\begin{bmatrix} \tilde{\mathbf{u}}_i^2 & \hat{\mathbf{K}} \\ \star & \hat{P} \end{bmatrix} > 0 \,\forall\, i = 1, 2. \tag{84}$$

where $\tilde{\mathbf{u}}_i$ denotes the peek control value of the i-th control input signal for every trajectory inside the domain of attraction $\mathcal{R}$.

Hence, one must simply include the LMI (84) into the optimization problem (82) in order restrict the peek value of each control input.

4. NUMERICAL EXAMPLE

This section presents a numerical simulation of two degrees of freedom manipulator control systems to illustrate the contribution presented in this paper. The numerical results were obtained in the MATLAB R2012b software and its native LMILAB toolbox was employed to solve the proposed convex optimization problem with LMI constraints.

An ideal two-link manipulator as shown in figure 1 is here considered with dynamics governed by (1), where the constructive parameters are $m_1 = 2\,\mathrm{kg}$, $m_2 = 1\,\mathrm{kg}$, $\ell_1 = 1\,\mathrm{m}$, $\ell_2 = 1\,\mathrm{m}$. The system has a reference signal $[\sin(\omega_f t) \ -\sin(\omega_f t)]^T$ with $\omega_f = 1\,rad/s$. Also the residual dynamics d were calculated by using a appropriated Taylor series approximation for the cases $p = 0$ and $p = 1$. Finally variable $\tau_2 = 0.5$ was selected in advance.

To illustrate the effect of the internal model on the steady-state error, the control design task has been done for the cases previously presented. Figure 2 presents the transient response, steady-state response, and the input signal to the different scenarios. It can be observed that the high order internal model leads to smaller error in the steady-state response due to the cancellation of the selected harmonics.

The robustness of the controller can be observed by the introduction of a additional load to the system, considering $\delta_m = 2$ when $t \geq 70s$ for the case where $p = 0$ as show in Figure (3).

Given these setup parameters, the proposed convex optimization problem yielded the feedback matrix:

$$\mathbf{K} = [K \ \boldsymbol{\Theta}], \tag{85}$$

with K and $\boldsymbol{\Theta}$ as presented in Table 1.

5. CONCLUSION

This paper proposed a systematic framework to achieve output regulation for a robotic manipulator system with two degrees of freedom. The steady-state conditions for the input were obtained by the so-called internal model approach which guarantees robustness to the system uncertain load mass. Furthermore, the stabilizing components that lead the system states to the steady-state manifold were synthesized through a convex optimization problem subject to LMI constraints.

Table 1. Controllers Gains

		(p=0)	(p=1)
K^T	$10^4 \times$	$\begin{bmatrix} -0.2142 & -0.0019 \\ 0.0214 & -0.2062 \\ -0.0735 & 0.0041 \\ 0.0121 & -0.0717 \end{bmatrix}$	$10^5 \times \begin{bmatrix} -0.0299 & -0.0003 \\ 0.0020 & -0.0288 \\ -0.0075 & 0.0003 \\ 0.0009 & -0.0073 \end{bmatrix}$
$\boldsymbol{\Theta}^T$	$10^4 \times$	$\begin{bmatrix} 1.3285 & -0.0092 \\ -0.1492 & 1.2670 \\ -0.9235 & -0.0558 \\ 0.0535 & -0.9192 \\ 0.6630 & -0.0069 \\ -0.0726 & 0.6183 \\ -0.2750 & -0.0104 \\ 0.0227 & -0.2758 \end{bmatrix}$	$10^5 \times \begin{bmatrix} 5.2046 & 0.0127 \\ -0.3789 & 4.9630 \\ -2.4535 & -0.1197 \\ 0.0930 & -2.4719 \\ 3.7261 & 0.0126 \\ -0.2536 & 3.4817 \\ -1.0150 & -0.0243 \\ 0.0671 & -1.0389 \\ 0.2264 & 0.0020 \\ -0.0131 & 0.2060 \\ -0.0599 & -0.0006 \\ 0.0048 & -0.0613 \end{bmatrix}$

Since this paper was mainly focused on the model of a planar two-link robotic manipulator, future work might explore the framework presented to higher-order dynamics. Beyond that, the study of other exogenous disturbances such as gravity could be a possibility.

REFERENCES

Castro, R.d.S. (2019). Output regulation of rational nonlinear systems with input saturation.

Castro, R.S., Flores, J.V., and Salton, A.T. (2022). Robust practical output regulation of rational nonlinear systems via numerical approximations to the regulator equations. *International Journal of Robust and Nonlinear Control*.

Chen, C., Zhang, C., Hu, T., Ni, H., and Luo, W. (2018). Model-assisted extended state observer-based computed torque control for trajectory tracking of uncertain robotic manipulator systems. *International Journal of Advanced Robotic Systems*, 15(5), 1729881418801738.

Chen, Z. and Huang, J. (2015). Stabilization and regulation of nonlinear systems. *Cham, Switzerland: Springer*.

Isidori, A., Marconi, L., and Serrani, A. (2003). *Robust autonomous guidance: an internal model approach*. Springer Science & Business Media.

Kumar, J., Kumar, V., and Rana, K. (2018). Design of robust fractional order fuzzy sliding mode pid controller for two link robotic manipulator system. *Journal of Intelligent & Fuzzy Systems*, 35(5), 5301–5315.

Kumar, J., Kumar, V., and Rana, K. (2020). Fractional-order self-tuned fuzzy pid controller for three-link robotic manipulator system. *Neural Computing and Applications*, 32(11), 7235–7257.

Muñoz-Vázquez, A.J., Gaxiola, F., Martínez-Reyes, F., and Manzo-Martínez, A. (2019). A fuzzy fractional-order control of robotic manipulators with pid error manifolds. *Applied soft computing*, 83, 105646.

Saraiva, E.S., Castro, R.S., Salton, A.T., and Pimentel, G.A. (2020). A convex optimization based solution for the robotic manipulator control design problem subject to input saturation. *IFAC-PapersOnLine*, 53(2), 5467–5472.

Trofino, A. and Dezuo, T. (2014). LMI stability conditions for uncertain rational nonlinear systems. *International Journal of Robust and Nonlinear Control*, 24(18), 3124–3169.

Yi, S. and Zhai, J. (2019). Adaptive second-order fast nonsingular terminal sliding mode control for robotic manipulators. *ISA transactions*, 90, 41–51.
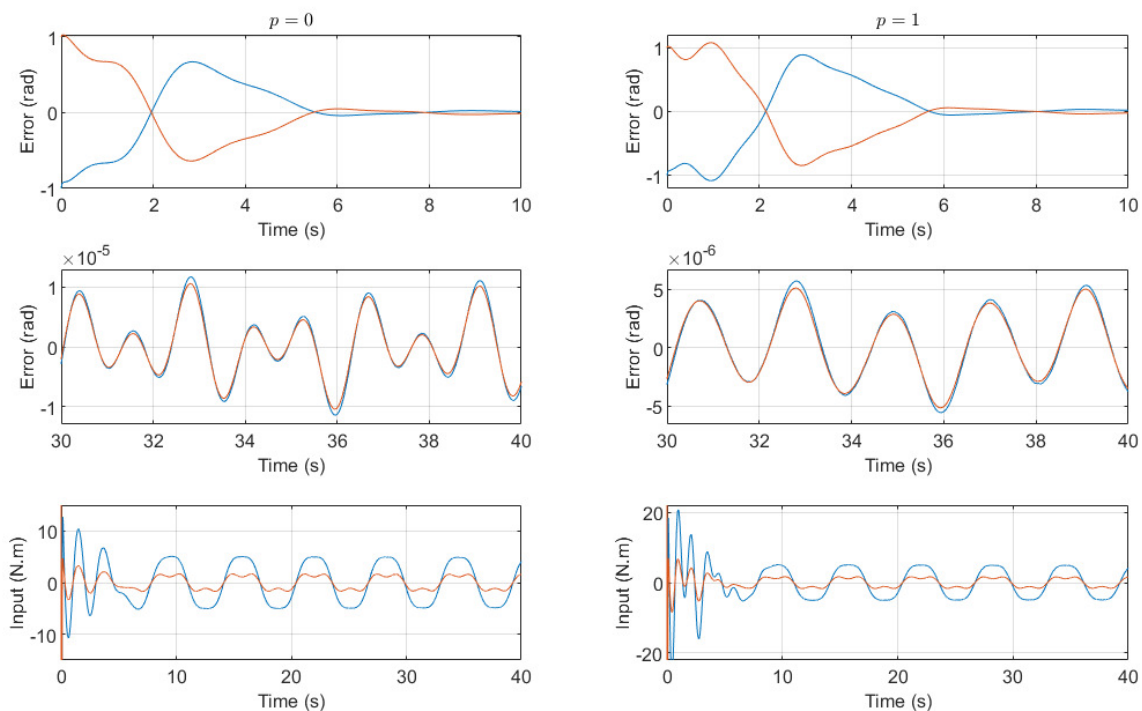
Figure 2. Comparison of the transient response, steady-state error and input signals between the different scenarios.
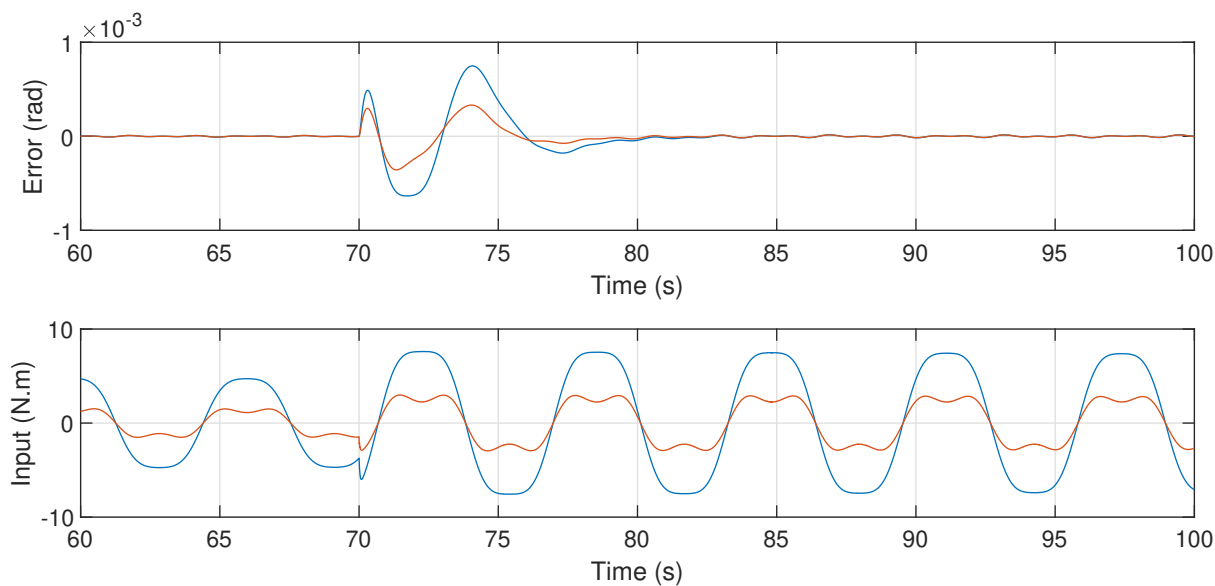
Figure 3. Comparison of the error signal and input signal when subjected to the uncertainty δ_m for $p = 0$.